

3. SITE 1152¹

Shipboard Scientific Party²

PRINCIPAL RESULTS

Site 1152 lies within a broad (2 km wide) valley in normal seafloor terrain of Segment B4. The seafloor age is ~25 Ma. Our choice of this site to begin Leg 187 operations was based on the assumption that it lies within the Indian Ocean mantle province. It would, therefore, provide an initial datum for a west-east traverse designed to locate the Indian/Pacific mantle boundary in the northern part of our operational area. The onboard geochemical results do not, however, unequivocally identify Indian-type mantle at this site.

Although the site-survey seismic profile showed a well-defined 2-km-wide sediment pond at least 75 m thick, we encountered hard rock in Hole 1152A almost immediately and abandoned the hole after only 11 m penetration into an unstable rubble pile. Most of the recovered material was fracture-bounded aphyric basalt talus defined as a single lithologic unit. In Hole 1152B, located only 100 m to the north-northeast, we encountered hard basement at ~20 meters below seafloor (mbsf) and continued through unstable conditions until it was abandoned at ~40 mbsf. In this hole, too, we seem to have encountered loose pillow basalt talus. Two lithologic units were defined: an upper, aphyric pillow basalt, which differed in its petrography and chemistry from that of Hole 1152A, and a lower, sparsely to moderately plagioclase-clinopyroxene pyritic pillow basalt. Basalts of both holes were slightly altered to clays and Fe oxyhydroxides.

Four whole-rock powders and three handpicked glasses were analyzed on board by inductively coupled plasma-atomic emission spectrometry (ICP-AES). The rock powders were also analyzed by X-ray fluorescence (XRF). All Site 1152 basalts are moderately evolved with <7.5 wt% MgO. The glasses have significantly higher MgO than the whole rocks, but their compositional differences cannot be explained by simple low-pressure crystal fractionation.

¹Examples of how to reference the whole or part of this volume.

²Shipboard Scientific Party addresses.

Relative to 0- to 5-Ma glasses from the same segment (Australian Antarctic Discordance [AAD] Segment B4), Site 1152 lavas are more evolved and appear to have been derived from a mantle source of somewhat different composition by a generally higher extent of melting. The latter observation may reflect shallower axial depths at ~25 Ma, consistent with the location of this site to the west of the depth anomaly.

Our expectation that this would prove to be a baseline Indian site appears to have been in error. On the Ba vs. Zr/Ba diagram, Site 1152 lavas are of Transitional-Pacific type (see “**Barium and Zirconium**,” p. 13, in “Geochemistry” in the “Leg Summary” chapter), a type not represented in our 0- to 7-Ma dredged sample collection.

OPERATIONS

Port Call

Fremantle

Leg 187 began at 1815 hr on 16 November 1999 when the first line was passed ashore to Berth H of Victoria Quay at Fremantle, Australia, at the conclusion of Leg 186ST. During the port call, several pieces of scientific apparatus were serviced (microscopes, XRF spectrophotometer, and cryogenic magnetometer), and the new ICP spectrophotometer was installed in the chemistry laboratory. The Ryan Energy Technology Fusion rig instrumentation software installation, which was started in Singapore during the dry dock, was also completed. The drill crew finished the assembly and static testing of the passive and active components of the heave compensator by the morning of 21 November. The project was complicated by the discovery that a defective directional servo valve in the active compensator required replacement. A local Bosch supplier expedited a replacement part from Adelaide during the evening of 20 November. Our departure was also delayed because the Fremantle tugboat operators conducted a 48-hr work stoppage starting the morning of 19 November and lasting until 0900 hr on 21 November.

At 1210 hr on 21 November, the last line was released from the pier and the *JOIDES Resolution* (JR) was maneuvered into the channel. After the pilot departed the vessel at 1300 hr, the JR began steaming at full speed on a southerly course.

Test Site

Transit to Test Site

Before proceeding to the first location of the leg, the ship was required to make a small diversion to a site off Albany in southwestern Australia. This was done in order to perform acceptance testing of the newly installed active heave compensator and the Fusion rig instrumentation system. The brief testing period also allotted additional time for crew familiarization with the new systems. The 401-nmi journey was completed at an average speed of 9.6 kt in calm seas and under fair skies.

Test Site: Albany, Western Australia

The 1-day testing program began at 0615 hr on 23 November with the deployment of a positioning beacon in ~285 m of water. Once the vessel stabilized over the beacon, the active heave compensator and the Fusion rig instrumentation were tested during mock coring exercises. Tony Muir, the Maritime Hydraulics representative, demonstrated the seafloor landing capabilities of the active heave compensator for the drilling crew during hands-on training exercises. John Grow, the Ryan Energy Technology representative, introduced the features and demonstrated the operation of the rig floor display to both drilling crews.

The testing exercise was completed in the early hours of the next morning. Once the drill string and beacon were recovered, the vessel sailed ~22 nmi to a prearranged rendezvous point between Breaksea Island and Bald Head at the mouth of Albany harbor. The *M/V Avon* came alongside at 0745 hr; Tony Muir, John Grow, Derryl Schroeder from the Ocean Drilling Program/Texas A&M University (ODP/TAMU), and Stefan Stan (representing Siemens) boarded the *Avon*. By 0800 hr on 24 November, the JR was under way at full speed to the first site of Leg 187.

Site 1152

Transit to Site

The 616-nmi transit to Site 1152 was accomplished at an average speed of 11.8 kt. The vessel rode well in a combined sea/swell of 10 ft. There was an occasional burst of wind-driven spray over the bow as the ship proceeded on a southeasterly heading. The skies were overcast with good visibility. At 0800 hr on 26 November, the vessel slowed to 6 kt while the seismic equipment was deployed. The objective was to conduct a single-channel seismic (SCS) survey across the precruise survey line. Data obtained from the survey were used to find localized sediment cover. An initial review of the seismic record suggested a sediment layer possibly 70 m thick overlying basement.

Site 1152

By noon, a north-to-south seismic line was concluded and the seismic equipment retrieved. The vessel came about and slowly approached the location. A beacon was dropped on the prospectus Global Positioning System (GPS) coordinates at 1215 hr. After the hydrophones and thrusters were extended and the vessel settled on the location, the corrected precision depth recorder (PDR) depth referenced to the dual elevator stool was 5066.4 m. A nine-collar bottom-hole assembly (BHA) was made up, comprising a C-4 four-cone rotary bit, a mechanical bit release, a head sub, an outer core barrel, a top sub, a head sub, seven 8¼-in drill collars, one tapered drill collar, six 5½-in drill pipes, and one crossover sub. Although no logging was anticipated, the mechanical bit release was affixed as a means of freeing the BHA should the drilling assembly become stuck at the bit.

Hole 1152A

Hole 1152A was spudded with the rotary core barrel (RCB) at 0830 on 27 November (Table T1). The bit tagged the seafloor at 5066.4 m. Instead of coring into a sediment pond, the bit appeared to contact hard rock immediately. After RCB coring 11 m with slow penetration and high and erratic torque, we decided to again attempt to contact

sediment by offsetting the vessel upcurrent of the present location. The vessel was repositioned in dynamic positioning mode ~100 m north-northeast of Hole 1152A.

Hole 1152B

Hole 1152B was spudded at 1330 hr and was washed ahead to 22.6 mbsf where we encountered a hard contact. Rotary coring was initiated in basalt at this sub-bottom depth and advanced to 40.6 mbsf with low recovery. At this depth, the drill string stuck and stalled the top drive. The driller worked for 1.25 hr to free the drill pipe with overpulls as large as 100,000 lb to regain control of the situation. After freeing the drill string, the interval from 40.8 to 45.3 mbsf was cored with improving recovery (28%). The bit was only advanced 1 m to 46.3 mbsf when the drill string stuck again. This time the drill pipe was freed with 40,000 lb of overpull. It was obvious at this juncture that the hole was too unstable to deepen, so coring operations were abandoned. The bit cleared the seafloor at 1500 hr and cleared the rotary table at 2345 hr on 28 November. Concurrent with the retrieval of the drill string, the beacon was successfully recovered. After the thrusters and hydrophones were retracted and the drilling equipment secured, the vessel was under way to the next site by 0000 hr on 29 November.

The average recovery of the site was 12%, providing adequate material to attain our scientific objectives. During the operations at this site, the environment was very mild for this region, with vessel heave not exceeding 2 m.

IGNEOUS PETROLOGY

Introduction

Volcanic rocks were encountered in Holes 1152A and 1152B at <1 and 22.6 mbsf, respectively. The drill holes penetrated what is interpreted as a talus pile composed of pillow basalt clasts. This interpretation is based on the absence of lithologic contacts, subangular shapes of clasts, and the predominance of weathered rinds or planar fracture surfaces on the majority of pieces (see "[Alteration](#)," p. 7). Thus, no primary magmatic stratigraphic significance can be associated with the position of individual pieces in the holes. Nonetheless, similarities in rock type justified grouping the rocks into distinct lithologic units. In Hole 1152A, 0.6 m (5% recovery) of light gray, aphyric basalt was recovered and designated as Unit 1. Total recovery for Hole 1152B was 3.6 m (15% recovery), and the material was divided into a unit of aphyric basalt and a unit of sparsely to moderately plagioclase-clinopyroxene phyric basalt. No lithologic contact was recovered, and the unit boundary in Hole 1152B was defined between Pieces 5 and 6 in Section 187-1152B-4R-1 on the basis of a marked change in phenocryst content. The lithologic units identified are summarized in [Table T2](#) and described below.

T2. Lithologic units summary, p. 28.

Hole 1152A

Unit 1

All of the core recovered in Hole 1152A has been assigned to a single lithologic unit. This unit is a light gray aphyric basalt and is slightly altered throughout (see "[Alteration](#)," p. 7). Small vesicles, typically <1

mm in size, are uniformly distributed and make up ~3% of the rock. Rare plagioclase phenocrysts (<<1%) as large as 2.5 mm are present in clusters (glomerocrysts); the crystals have rounded (partially resorbed?) shapes, are twinned, and display a fine-scale oscillatory zoning. Skeletal to subhedral olivine microphenocrysts as large as 0.8 mm are present as discrete crystals and in association with lath-shaped plagioclase microphenocrysts. Phenocrysts and microphenocrysts are unaltered.

Thin sections show that the microcrystalline groundmass consists of quench textures, ranging from sheaf to plumose, though sheaf textures predominate (Fig. F1). The sheafs consist mainly of acicular to skeletal plagioclase intergrown with plumose quench clinopyroxene. Proportions of groundmass phases are difficult to estimate because of the predominance of cryptocrystalline quench morphologies, but plagioclase content is probably greater than clinopyroxene, both of which are significantly more abundant than olivine. Dark brown interstitial material (altered glass + quench phases?) makes up ~10% of the rock, and minute (<20 μm) equant opaque minerals make up 1%–2% of the groundmass; ~1% of the opaque minerals are 2- to 3- μm pyrite globules. Alteration is usually restricted to localized replacement of groundmass by Fe oxyhydroxides and a more pervasive, although still minor, replacement of groundmass by smectite. Vesicles are also filled with smectite.

Glassy rinds were recovered on four pieces of the core (Table T3). The most complete rind (Sample 187-1152A-1R-1 [Piece 8]) consists of a thin layer (1–2 mm thick) of clear, dark brown glass containing plagioclase microlites and a few dispersed spherulites, followed inward by a wider zone of light gray, coalesced spherulites (~5 mm wide). This is followed in turn by a light brown spherulitic zone that is at least 1 cm wide and texturally grades into the more fully crystallized interior of the rock. The widths of the coalesced spherulite and spherulitic zones in Sample 187-1152A-1R-1 (Piece 8) are typical of those observed elsewhere at Site 1152 (e.g., see Sample 187-1152B-5R-1 [Piece 25] in Fig. F2). For most samples from Hole 1152A, clear glass was not recovered, and the glassy rinds begin with the zones of coalesced spherulites (Table T3).

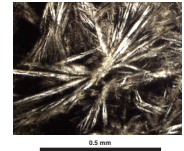
The presence of high-angle intersecting fractures in Sample 187-1152A-1R-1 (Piece 3) probably explains the distinct V shapes of many fragments at Site 1152. These are radial fractures typical of pillow lavas.

Hole 1152B

Unit 1

Unit 1 of Hole 1152B is an aphyric basalt macroscopically similar to the aphyric basalt of Hole 1152A, although petrographic observations and geochemistry indicate that these are distinct units. Unit 1 of Hole 1152B contains <1% plagioclase microphenocrysts, most of which are <1 mm. In contrast, olivine microphenocrysts have not been observed, and clinopyroxene (as large as 0.2 mm) constitutes a larger proportion of the groundmass. In thin section, the groundmass texture is quite variable, ranging from sheaf and plumose quench textures (Fig. F3) to intersertal (Fig. F4) and even subophitic in more coarse-grained areas. Smaller groundmass plagioclase crystals (<0.5 mm) are acicular to skeletal, but larger microphenocrysts are prismatic to tabular and contain pockets of devitrified glass (Fig. F5). In most cases, these glass pockets have irregular shapes, which suggests they have formed by partial re-

F1. Plagioclase sheaf quench texture, p. 13.

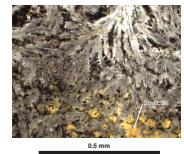


T3. Glass occurrences summary, p. 29.

F2. Progression from a chilled pillow margin into a holocrystalline interior, p. 14.



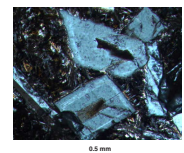
F3. A clinopyroxene plumose quench texture, p. 15.



F4. An intersertal groundmass texture, p. 16.



F5. Partially resorbed plagioclase microphenocrysts, p. 17.



sorption of the plagioclase. Some larger microphenocrysts display oscillatory zoning, whereas most groundmass plagioclase is either unzoned or normally zoned.

Proportions of groundmass phases are difficult to estimate because of the predominance of cryptocrystalline quench morphologies, but clinopyroxene is probably equal to or greater than plagioclase in abundance. Dark brown interstitial material (altered glass + quench phases?) makes up ~15% of the rock. Minute (<30 μm) equant to acicular opaque minerals make up ~3% of the groundmass. Pyrite globules (<2 μm) constitute only a trace proportion (<<1%) of the opaque minerals. Small vesicles, typically <1 mm, are variably distributed throughout and make up between 2% and 5% of the rock.

The rocks are slightly altered, with alteration concentrated toward outer surfaces of pieces or along fractures (see “**Alteration**,” p. 7). In thin section, alteration appears as patchy replacement of groundmass by Fe oxyhydroxides and smectite. Some smectite patches have a distinctive diamond shape, which may indicate replacement of groundmass olivine, but these apparent pseudomorphs are uncommon, and fresh olivine has not been observed. Most vesicles are also filled with smectite.

Eight pieces of core from this unit include glassy rinds or fragments (Table T3). For most pieces, the glass consists of coalesced spherulites (i.e., clear glass is not present). The most complete glass rind for this unit (Sample 187-1152B-3R-1 [Piece 1]) displays the same sequence of quench zones as Sample 187-1152A-1R-1 (Piece 8), described above, although the amount of clear glass recovered with Sample 187-1152A-3R-1 (Piece 1) is significantly larger (as thick as 1 cm). Sample 187-1152B-2R-1 (Piece 4) is a unique occurrence in which the glass (~2 mm thick) is incorporated as a relatively unaltered tabular fragment within layers of palagonite and a sedimentary crust composed of Mn oxides and pelagic sediment.

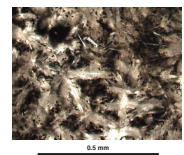
Unit 2

Unit 2 in Hole 1152B is a sparsely to moderately plagioclase-clinopyroxene phyric basalt that is slightly altered. Prismatic to tabular, subhedral plagioclase phenocrysts range from 1 to 4 mm and make up 2%–5% of the rock. Subhedral to anhedral clinopyroxene phenocrysts (1–6 mm) constitute 1%–3% of the rock. Subhedral olivine phenocrysts (0.5–4 mm) are present throughout, although their abundance is usually <1%.

Olivine phenocrysts are partially replaced by iddingsite, but other phenocryst phases tend to be free of alteration. Clinopyroxene phenocrysts are present as discrete crystals and in association with plagioclase as glomerocrysts. Plagioclase + olivine glomerocrysts are also present. Plagioclase in glomerocrysts tend to display complex oscillatory zoning and to contain pockets of devitrified glass, probably because of partial resorption. In addition, both clinopyroxene and plagioclase phenocrysts commonly have quench overgrowths.

In thin section, the groundmass texture is dominated by immature plumose quench textures (Fig. F6), with as much as 5% acicular to skeletal plagioclase crystals (<0.2 mm). As with the other lithologic units at Site 1152, the proportions of groundmass phases are difficult to estimate because of the predominance of cryptocrystalline quench morphologies. However, based on the predominance of plumose quench textures, there is probably more clinopyroxene than plagioclase.

F6. Immature clinopyroxene plumose quench textures, p. 18.



Minute (<20 μm) equant to acicular opaque minerals make up ~1%–2% of the groundmass; ~1% of the opaque minerals are tiny (~2 μm) pyrite globules. Vesicles constitute 2%–3% of the rock and are typically <1 mm in diameter, although some as large as 3 mm were observed. Vesicles tend to be filled with smectite only in distinct zones of alteration (see “Alteration,” p. 7) toward the rims of pieces.

Glassy rinds or fragments were recovered on nine pieces of core from this unit (Table T3). In contrast to the glassy rinds from the two aphyric units, all of the rinds recovered in Unit 2 contain at least some clear glass. Sample 187-1152B-5R-1 (Piece 25) is typical (Fig. F2).

ALTERATION

Basalts recovered from Holes 1152A and 1152B are generally slightly altered but show variable degrees of alteration within individual pieces. Macroscopically, alteration seems to be confined to coatings, vesicle fillings, veins, fractures, and distinctive concentric zones a few millimeters to several centimeters in width. Clay minerals (smectite), Fe oxyhydroxides, and cryptocrystalline silica are the predominant secondary minerals. These minerals occur as fillings of vesicles, fractures, and veins. Alteration minerals of the groundmass include smectite and Fe oxyhydroxide, which commonly replace clinopyroxene and olivine. Small (<1 mm) spots of Mn oxide are present on the weathered surfaces of basalt fragments from Hole 1152B. A crust consisting of dendritic textured Mn oxide interfingering with pelagic sediment is present near the top of Unit 1 in Hole 1152B (Fig. F7). In the same section, XRD analysis of a vein (Sample 187-1152B-2R-1 [Piece 1]) reveals the presence of smectite and minor quartz.

Distinctive concentric alteration halos follow the shape of the outer surfaces of individual basalt pieces from Hole 1152B. These zones usually have sharp smooth contacts with the less altered interior, although in some pieces they are more gradational and irregular (e.g., Section 187-1152B-6R-1 [Piece 5]; Fig. F8). Based on color, texture, abundance of secondary minerals, filling of vesicles, and apparent differences in crystallinity, two distinct alteration zones can be distinguished both macroscopically and microscopically:

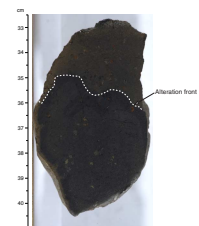
1. The outermost zone is light brown, 1–3 mm thick, and dominated by smectite and Fe oxyhydroxide. This type of alteration usually affects the original (predrilling) surfaces of basalt clasts, especially in the lower half of Unit 2 of Hole 1152B, and also occurs along fractures.
2. Adjacent to the outer zone is a light gray zone, which is usually 5–10 mm wide. In cut surfaces of hand specimens this zone appears to be aphyric and unaltered. However, under the microscope, plagioclase and olivine phenocrysts are visible and small vesicles (<0.5 mm) are seen to be completely filled by smectite. In some areas, the groundmass has been replaced by the same clay mineral; groundmass alteration decreases toward the interiors of pieces. Plagioclase phenocrysts appear unaffected by this alteration, but olivine phenocrysts are partially iddingsitized (Fig. F9).

The macroscopically sharp boundary separating the outer and inner zones has a more irregular character in thin section, manifested by a dis-

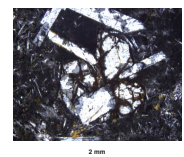
F7. Dendritic Mn oxide interfingering with pelagic sediment, p. 19.



F8. Concentric alteration halos, p. 20.



F9. Iddingsitized olivine and fresh plagioclase, p. 21.



tinct decrease in smectite alteration of the groundmass. The interior portions of each piece are medium gray and slightly vesicular; both groundmass and phenocryst phases are free of alteration. The distinct alteration halos are therefore interpreted to reflect low-temperature alteration fronts, progressing from the exterior and fracture surfaces to the center of each fracture-bounded basalt fragment. The degree of alteration varies with clast size, type of quench zone texture (such as spherulitic, sheaf, or plumose), and fracture density. The degree of alteration does not change with depth.

Rare glassy pillow rinds of 0.5–10 mm thickness were recovered from both Hole 1152A and 1152B. Within the rinds, glass ranges from fresh to completely altered. Fresh glasses are dark brown in thin section and shiny black in hand specimen. Altered glass (palagonite) is yellow to orange and has dull surfaces. Fresh glass and palagonite commonly occur in thin (0.5–2 mm), irregularly interlayered sheets, with palagonite being most abundant (>90%) in the outermost sections. Macroscopically, the boundary between fresh glass and palagonite is sharp; thus, alteration appears to have preferentially progressed along (cooling?) cracks.

MICROBIOLOGY

At Site 1152, two rock samples (187-1152A-1R-1 [Piece 1A, 0–5 cm] and 187-1152B-4R-1 [Piece 12, 71–78 cm]) were collected to characterize the microbial community inhabiting this environment (Table T4). Both samples are fragments of pillow lava, consisting of a partly altered glassy margin and some of the more crystallized interior. Core 187-1152A-1R has a partly weathered, yellowish brown surface with small black spots of Mn oxides.

Two approaches to minimize drilling-induced contamination on the outer sample surface were followed at this site. For Sample 187-1152A-1R (Piece 1A, 0–5 cm), the outer surface of the core was split off with a hydraulic rock trimmer, and the remaining pieces were used for experiments. This method exposes the sample to oxygen for 45–60 min, and obligate anaerobes were not expected to grow. Nevertheless, this sample was treated as an aerobic sample and was only inoculated in three aerobic media and two nonreduced anaerobic media. In the nonreduced media, facultative anaerobes may grow.

For Sample 187-1152B-4R (Piece 12, 71–78 cm), the outer surface was quickly flamed with an acetylene torch, which proved to be the simplest and fastest sterilization method. This minimized the time the rock sample was exposed to oxygen to 20 min. After the sterilization, enrichment cultures and samples for DNA analysis and electron microscope studies were prepared as described in “[Igneous Rocks](#),” p. 7, in “Microbiology” in the “Explanatory Notes” chapter.

SITE GEOPHYSICS

Leg 187 Site 1152 was located based on 1997-vintage single-channel seismic data, plus a short 3.5-kHz PDR and SCS survey conducted on approach to the site. Onboard instrumentation used included a precision echo sounder, gyrocompass, seismic system, and GPS receivers.

T4. Rock samples prepared for on-shore microbial studies, p. 30.

Echo Sounder

Both 3.5- and 12-kHz PDRs were used to acquire bathymetric data as well as high-resolution reflection records of the uppermost sediment layers.

Seismic Reflection Profiling

Site selection for the first drill site of Leg 187 (Site 1152) was based on a SCS survey conducted during *R/V Melville* cruise Sojourner 5 in 1997. A ~1.4-hr SCS survey was conducted on approach to Site 1152 (JR SCS line S1; Fig. F10) to ensure the correct site location by comparing the GPS-navigated SCS data with the 1997 SCS image. The ship's speed averaged 5.7 kt during the SCS survey. The water gun was triggered at a shot interval of 12 s, equivalent to ~35 m at 5.7 kt. Data acquisition and processing parameters were described in "Underway Geophysics," p. 10, in the "Explanatory Notes" chapter. There are several course changes in line S1 as the ship maneuvered to approach the site on a north-south line; the ship's heading was 130°, 160°, and 180° from ~02:20, 02:54, and 03:10, respectively. The final position of Site 1152 was shifted ~2.7 km south of the prospectus site AAD-36a to an apparently thicker sediment pond. We marked this position near seismic shot number 301 of line S1. The depth at the site is 5066.4 m (see Fig. F11), with sediment cover from 6.8 to 6.95 s two-way traveltime, estimated to be ~150 m. The 3.5-kHz analog data were used to confirm this selection.

GEOCHEMISTRY

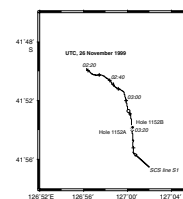
Introduction

Site 1152 basalts were recovered from ~25-Ma seafloor formed within spreading Segment B4 of the AAD. Four whole-rock powders were analyzed for major and trace elements by XRF and ICP-AES and three samples of fresh glass chips by ICP-AES only. The results are shown in Table T5. At this early stage in Leg 187, the ICP-AES results were poor for some elements because of dissolution problems and inexperience with the new JY2000 instrument. The major element data are the most compromised; SiO₂ could only be estimated by difference from 100% total oxides. This problem affects only the whole-rock ICP-AES analyses in Table T5; the glasses from Hole 1152 were reanalyzed during later ICP-AES runs. Only the XRF whole-rock data and ICP-AES glass data are shown on plots and considered in the discussion.

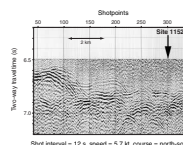
Holes 1152A and 1152B

Samples from Hole 1152A are assigned to a single aphyric basalt unit based on macroscopic and microscopic examination. These basalts are moderately evolved (i.e., <7.5 wt% MgO). The glass from Hole 1152A is distinctly higher in MgO (7.3 wt%) than the whole rocks (6.0–6.5 wt%; Fig. F12). The other major and trace element concentrations are offset from the glass compositions in directions that are generally orthogonal to expected low-pressure crystal fractionation trends. For example, whole-rock Al₂O₃ is higher for a given MgO content relative to associated glass rather than lower as removal of plagioclase and olivine would dictate. In addition, Cr, Zr, and Y contents of whole rocks are offset

F10. Track chart of single-channel seismic survey line S1, p. 22.

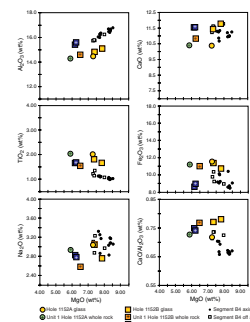


F11. Single-channel seismic record from *JOIDES Resolution* survey line S1, p. 23.



T5. Compositions of Site 1152 basalts, p. 31.

F12. Major element variations vs. MgO for basalts from Holes 1152A and 1152B, p. 24.



both from the glasses and from melt evolution trends defined by younger Segment B4 glass samples (Fig. F13). These observations suggest that alteration, particularly the selective removal of MgO and/or nonequilibrium differentiation, have affected the whole-rock compositions (see “Alteration,” p. 7).

Samples from Hole 1152B are assigned to two lithologic units: Unit 1 is an aphyric pillow basalt, and Unit 2 is a sparsely to moderately plagioclase-clinopyroxene phyric pillow basalt. The glasses from both units (undifferentiated in Figs. F12 and F13) are higher in MgO (7.6–8.0 wt%) than the whole rocks (6.2–6.9 wt%). The plagioclase-clinopyroxene phyric Unit 2 basalt has higher Al_2O_3 , CaO (Fig. F12), and Sr (Fig. F13) contents than the Unit 1 aphyric basalt, consistent with its phenocryst assemblage, which suggests plagioclase accumulation. Hole 1152B glasses appear to be genetically related by a typical low-pressure crystal fractionation path of decreasing Al_2O_3 , Cr, and Ni and increasing Fe_2O_3 , Na_2O , TiO_2 , Zr, and Y. Glass compositions from Holes 1152A and 1152B are distinctly different on the $\text{CaO}/\text{Al}_2\text{O}_3$ vs. MgO diagram, with those from Hole 1152B having higher $\text{CaO}/\text{Al}_2\text{O}_3$ values for a given MgO content than those from Hole 1152A (Fig. F12). As for samples from Hole 1152A, the relationships between glass and whole rocks from each unit cannot be attributed to simple low-pressure fractional crystallization and are more likely controlled by alteration of the whole rock and/or nonequilibrium differentiation, perhaps including variable amounts of plagioclase accumulation.

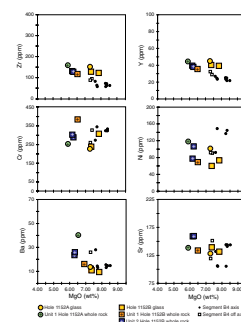
Temporal Variations

Whole rocks from Site 1152 lie beyond the more evolved end of the compositional range of 0- to 5-Ma mid-ocean-ridge basalt (MORB) from Segment B4. The glasses have MgO contents comparable to those of younger B4 glasses; however, they differ by having significantly lower Al_2O_3 , marginally lower Ba, and higher TiO_2 , Fe_2O_3 , Zr, and $\text{CaO}/\text{Al}_2\text{O}_3$ (Hole 1152B only) for a given MgO content. The shifts in some of these geochemical characteristics could indicate a temporal change in melting parameters beneath the Segment B4 spreading axis. Additional support for this can be seen in the off-axis dredge compositions, particularly the generally higher $\text{CaO}/\text{Al}_2\text{O}_3$ values relative to B4 axial lavas. Higher Fe_2O_3 and $\text{CaO}/\text{Al}_2\text{O}_3$ values and lower Ba content suggest a higher degree of melting beneath this segment in the past. This would be consistent with the inference that Segment B4 was shallower at 25 Ma than it is today because it was located west of the depth anomaly at that time. The mantle source must also differ in composition, mineralogy, and/or melt extraction process to explain the higher concentrations of moderately incompatible elements TiO_2 , Zr, and Y, since a simple increase in melting would be expected to lower the concentrations of these elements.

Mantle Domain

Site 1152 was selected as our initial site to provide a baseline Indian-type composition at ~30 Ma because no evidence exists to suggest Pacific-type mantle was ever west of the B5 spreading axis. This may prove to have been an erroneous assumption. The Zr/Ba systematics of Site 1152 basalts do not unequivocally assign this site to either the Indian or the Pacific mantle domain. All three glasses plot within a small re-

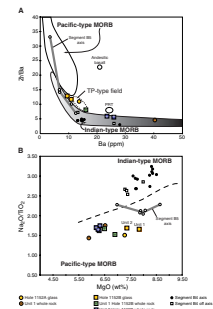
F13. Trace element variations vs. MgO for basalts from Holes 1152A and 1152B, p. 25.



gion that lies outside our predefined Indian and Pacific fields (Fig. F14A); they lie on the Pacific side of the trend defined by present-day transitional lavas from Segment B5 at lower Zr/Ba ratios than the predefined Pacific field. The whole-rock samples have more Ba and consequently lower Zr/Ba ratios, which could result from excess Ba introduced by seawater alteration, although results from subsequent sites suggest that there are consistent trends defined by spatially related glasses and whole rocks that cannot be explained solely by alteration.

The $\text{Na}_2\text{O}/\text{TiO}_2$ vs. MgO diagram (Fig. F14B), taken at face value, indicates a Pacific-type MORB source. On balance, it appears from the available data that Site 1152 lavas have at least some degree of Pacific affinity, if not truly a Pacific-type source. Little evidence, other than our initial expectations, suggests an Indian-type MORB source. As a general rule, where these two diagrams conflict, we consider that the Zr/Ba vs. Ba systematics are more reliable in determining source characteristics, as these trace elements are much less likely than TiO_2 and Na_2O to have been affected by crustal processes (e.g., boundary-layer fractionation) (Langmuir, 1989; Nielsen and Delong, 1992). We also recognize that, although Zr/Ba is demonstrably more reliable than $\text{Na}_2\text{O}/\text{TiO}_2$ for axial lavas, it is not unequivocal. Our shallow drill holes are sampling only the very last volcanic events before crust was transported off axis, and we may even be sampling off-axis magmatism. Lavas from such eruptions have been shown to be more diverse in some regions (Reynolds et al., 1992) and might be expected to have higher TiO_2 and, therefore, lower $\text{Na}_2\text{O}/\text{TiO}_2$ ratios, giving the impression of a Pacific-type affinity. The mantle domain for this site will not be resolved without isotopic data.

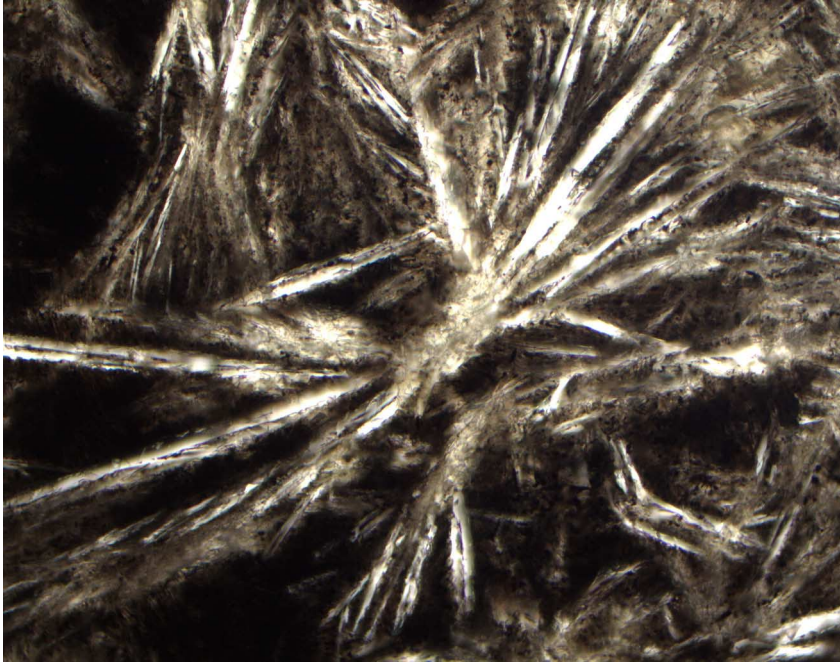
F14. Zr/Ba vs. Ba and $\text{Na}_2\text{O}/\text{TiO}_2$ vs. MgO for basalts from Holes 1152A and 1152B, p. 26.



REFERENCES

- Langmuir, C.H., 1989. Geochemical consequences of *in situ* crystallization. *Nature*, 340:199–205.
- Nielsen, R.L., and Delong, S.E., 1992. A numerical approach to boundary layer fractionation: application to differentiation in natural magma systems. *Contrib. Mineral. Petrol.*, 110:355–369.
- Reynolds, J.R., Langmuir, C.H., Bender, J.F., Kastens, K.A., Ryan, W.B.F., 1992. Spatial and temporal variability in the geochemistry of basalts from the East Pacific Rise. *Nature*, 359:493–499.

Figure F1. Photomicrograph in plane-polarized light of Sample 187-1152A-1R-1, 30–34 cm (see “[Site 1152 Thin Sections,](#)” p.9), showing a plagioclase sheaf quench texture.



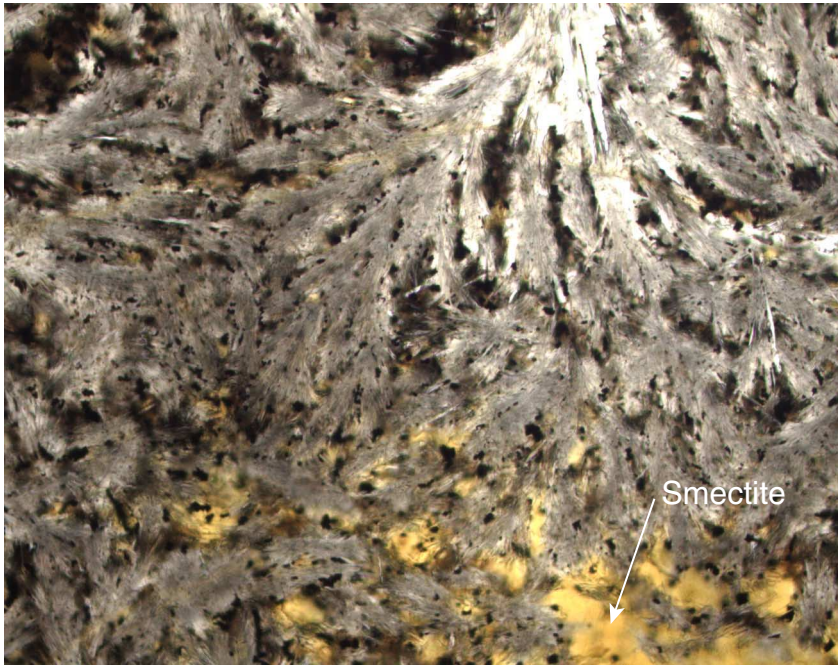
0.5 mm



Figure F2. Photograph of interval 187-1152B-5R-1 (Piece 25, 143–150 cm), showing the progression from a chilled pillow margin (dark gray to black area) into a holocrystalline interior (light gray area).



Figure F3. Photomicrograph in plane-polarized light of Sample 187-1152B-2R-1, 8–10 cm (see “[Site 1152 Thin Sections](#),” p.10), showing a clinopyroxene plumose quench texture. Note the replacement of ground-mass mesostasis by smectite (lower right).



0.5 mm



Figure F4. Photomicrograph of Sample 187-1152B-2R-1, 8–10 cm (see “[Site 1152 Thin Sections](#),” p.10), showing an intersertal groundmass texture. Long acicular to prismatic to tabular crystals are plagioclase. Equant anhedral crystals clustered around plagioclase are clinopyroxene. Dark patches are areas of mesotaxis.



0.5 mm

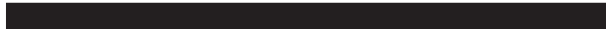
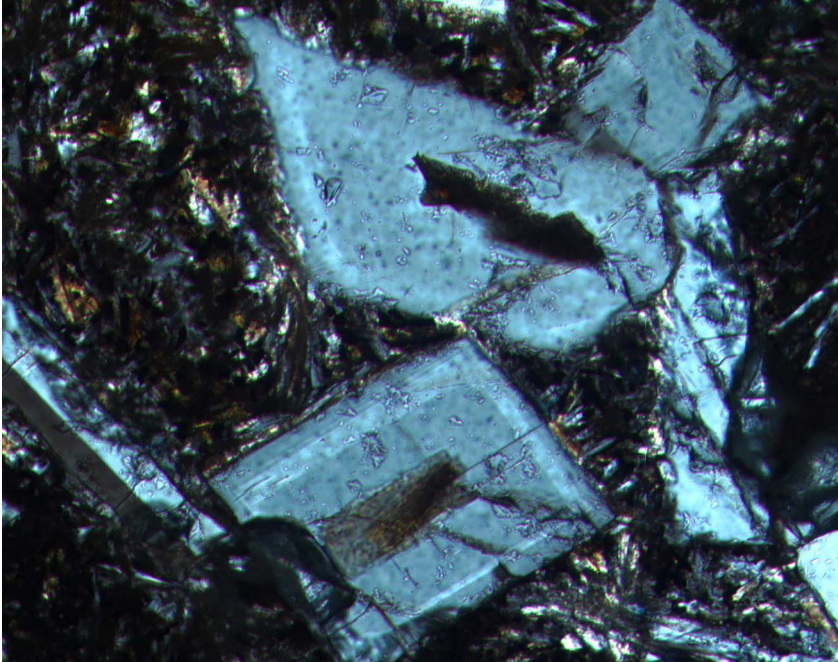


Figure F5. Photomicrograph, with crossed polars, of Sample 187-1152B-2R-1, 8–10 cm (see “[Site 1152 Thin Sections](#),” p.10), showing partially resorbed plagioclase microphenocrysts.



0.5 mm

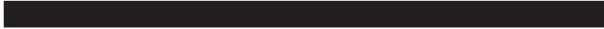
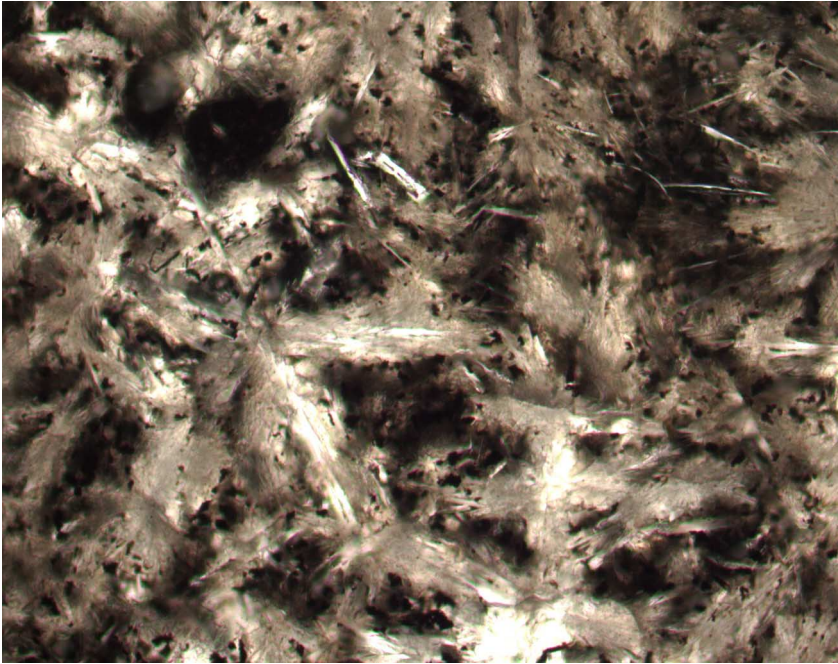


Figure F6. Photomicrograph in plane-polarized light of Sample 187-1152B-4R-1, 57–61 cm (see “[Site 1152 Thin Sections](#),” p.11), showing immature clinopyroxene plumose quench textures. Light, feathery clinopyroxene crystals are decorated with small black equant opaque minerals. Dark interstitial areas are mesostasis.



0.5 mm



Figure F7. Photograph of interval 187-1152B-2R-1 (Piece 4, 19–22 cm), showing dendritic Mn oxide inter-fingered with pelagic sediment, both attached to a strongly palagonitized pillow glass rind.

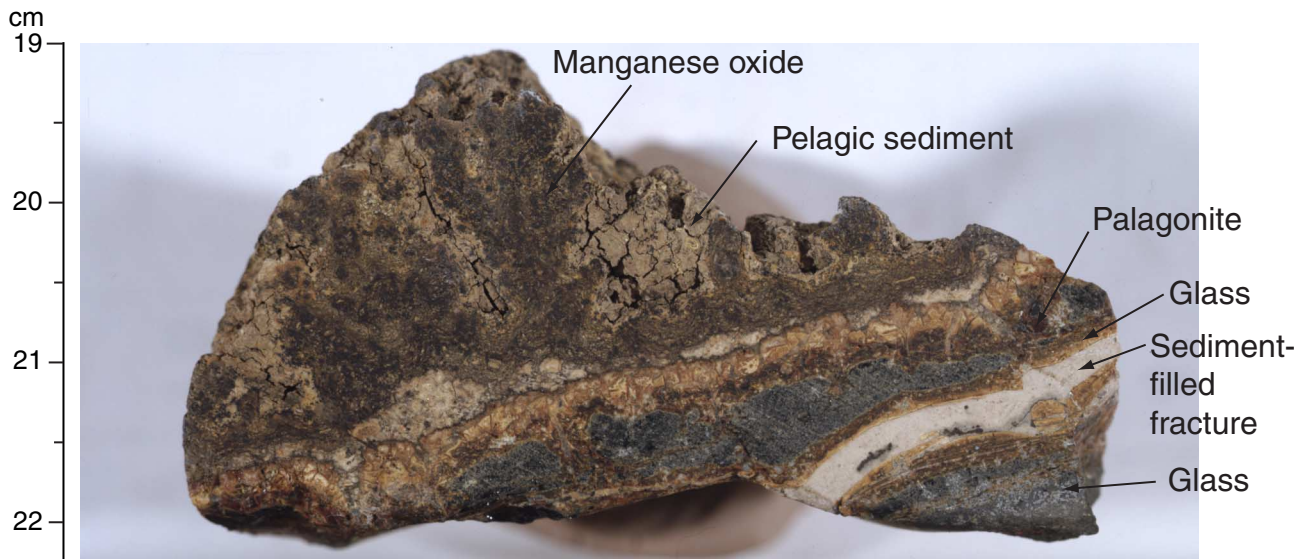


Figure F8. Photograph of interval 187-1152B-6R-1, 32.5–40.5 cm, showing concentric alteration halos progressing from more intensely altered margin to a less intensely altered interior of the piece.

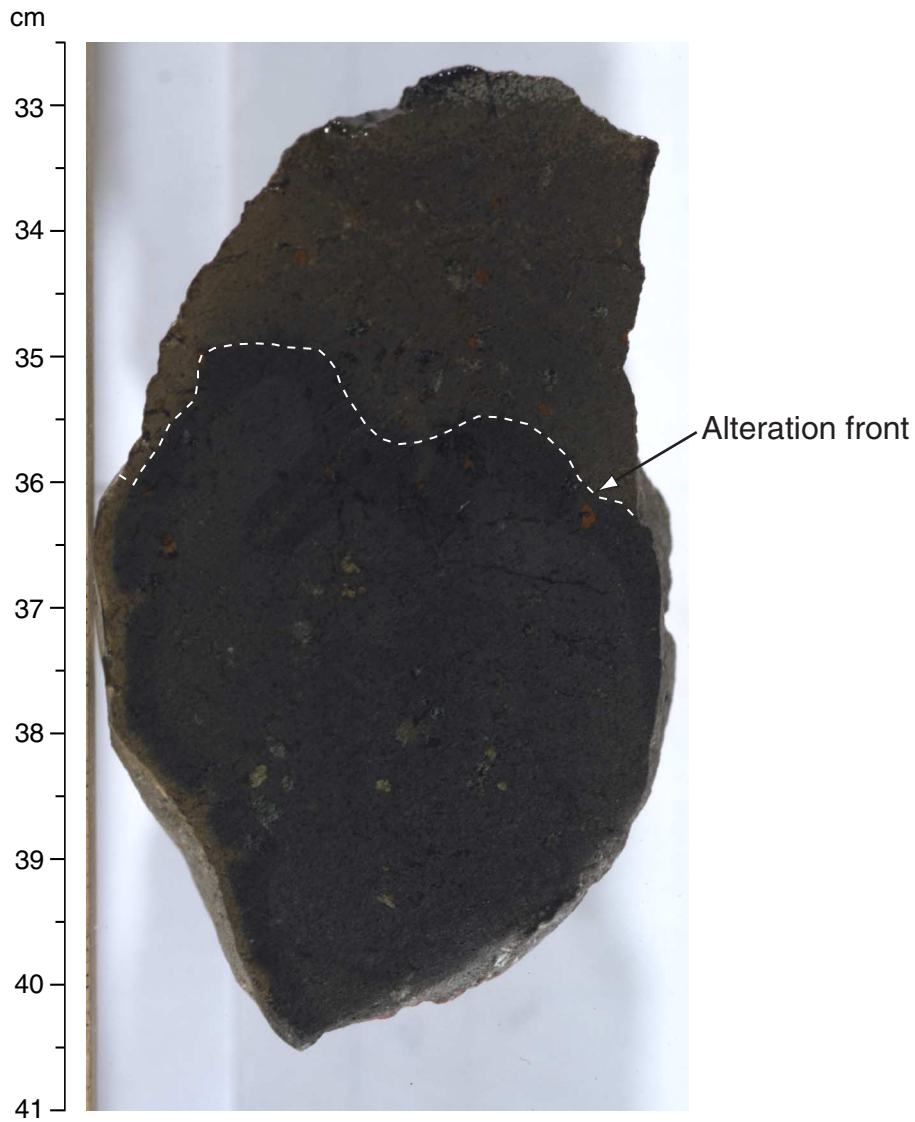
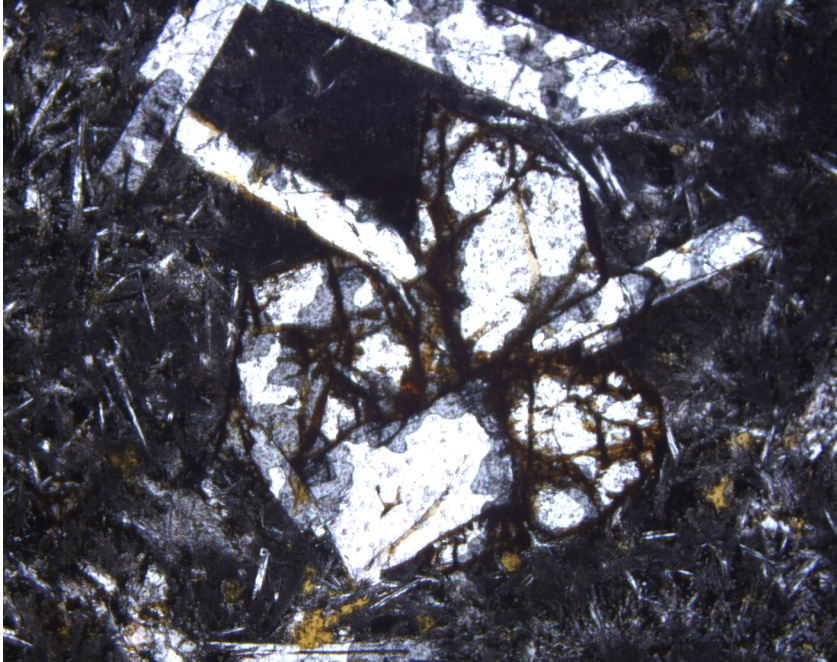


Figure F9. Photomicrograph, with crossed polars, of Sample 187-1152B-4R-1, 57–61 cm (see “[Site 1152 Thin Sections](#),” p. 11), showing iddingsitized olivine and fresh plagioclase.



2 mm



Figure F10. The track chart of the *JOIDES Resolution* single-channel seismic (SCS) survey line S1. UTC = Universal Time Coordinated; crosses = 10-min intervals; solid circles = Holes 1152A and 1152B; open circle = prospectus site AAD-36a. AAD = Australian Antarctic Discordance.

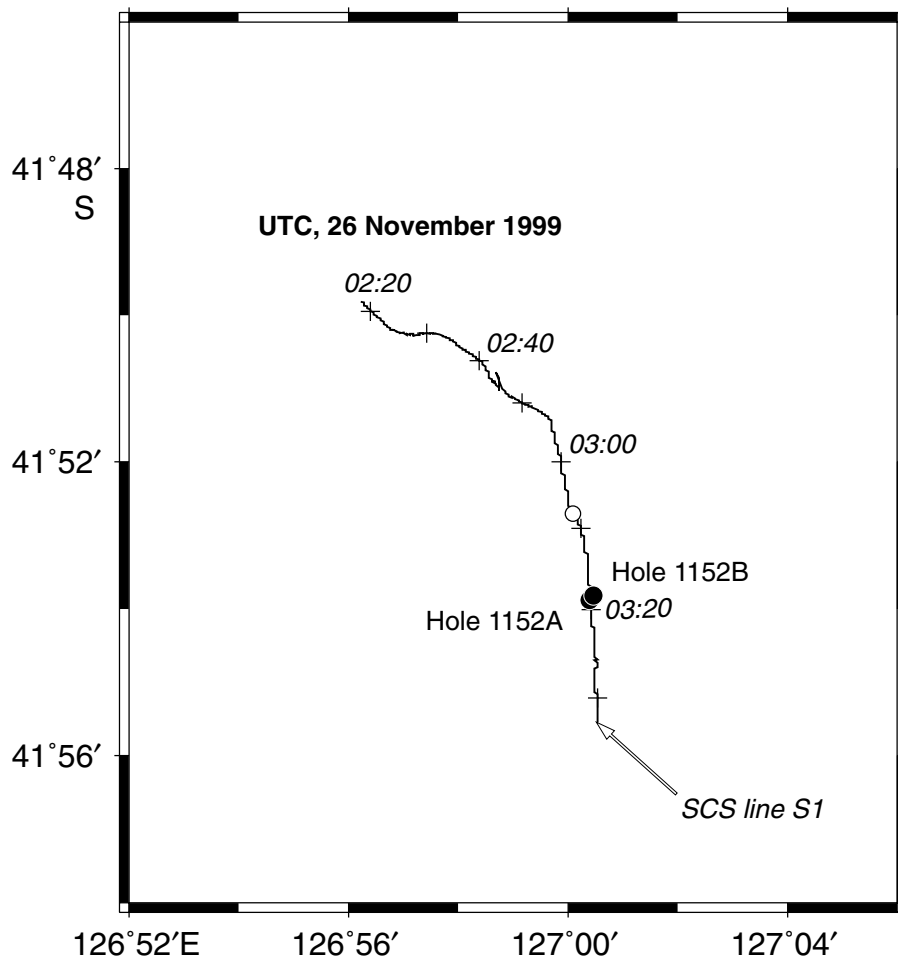
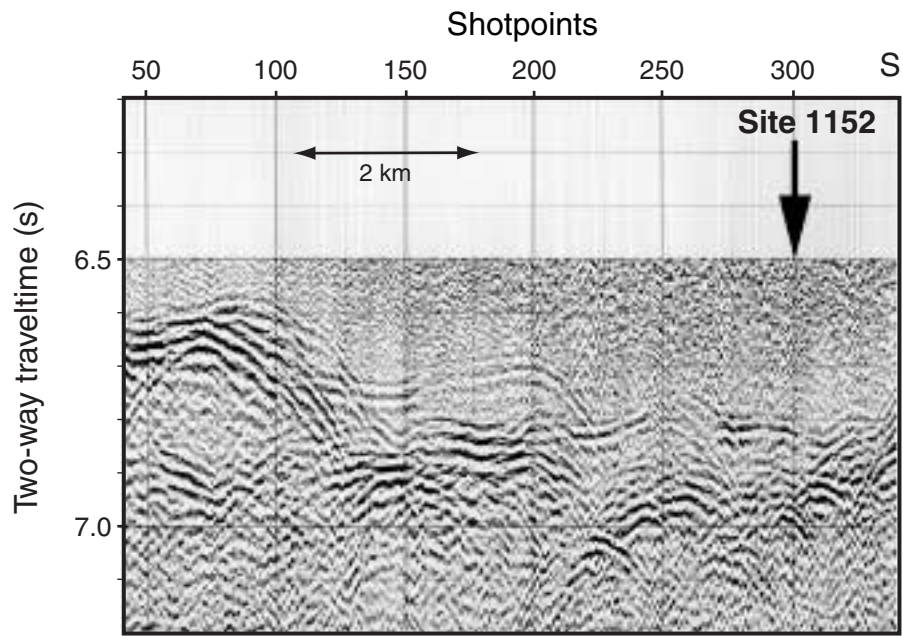


Figure F11. Single-channel seismic record from *JOIDES Resolution* survey line S1.



Shot interval = 12 s, speed = 5.7 kt, course = north-south

Figure F12. Major element variations vs. MgO for basalts from Holes 1152A and 1152B compared with Southeast Indian Ridge glasses from Segment B4. Only the averaged X-ray fluorescence data for whole rocks and ICP-AES data for glasses are shown. The ICP-AES data for whole-rock samples are not plotted.

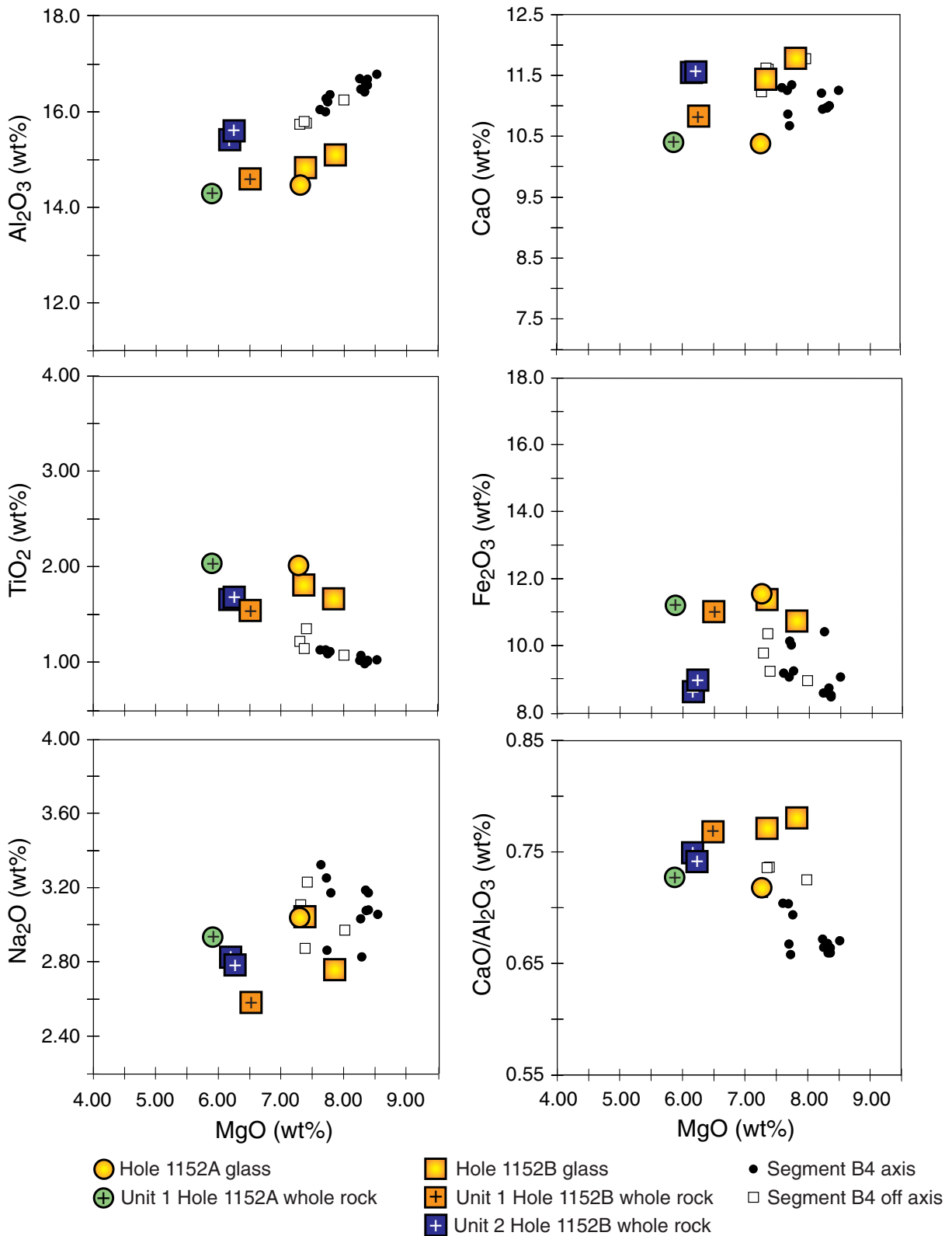


Figure F13. Trace element variations vs. MgO for basalts from Holes 1152A and 1152B compared with Southeast Indian Ridge glasses of Segment B4. The ICP-AES whole-rock data are not plotted for this site except on the Ba vs. MgO diagram, since Ba values are below detection for X-ray fluorescence.

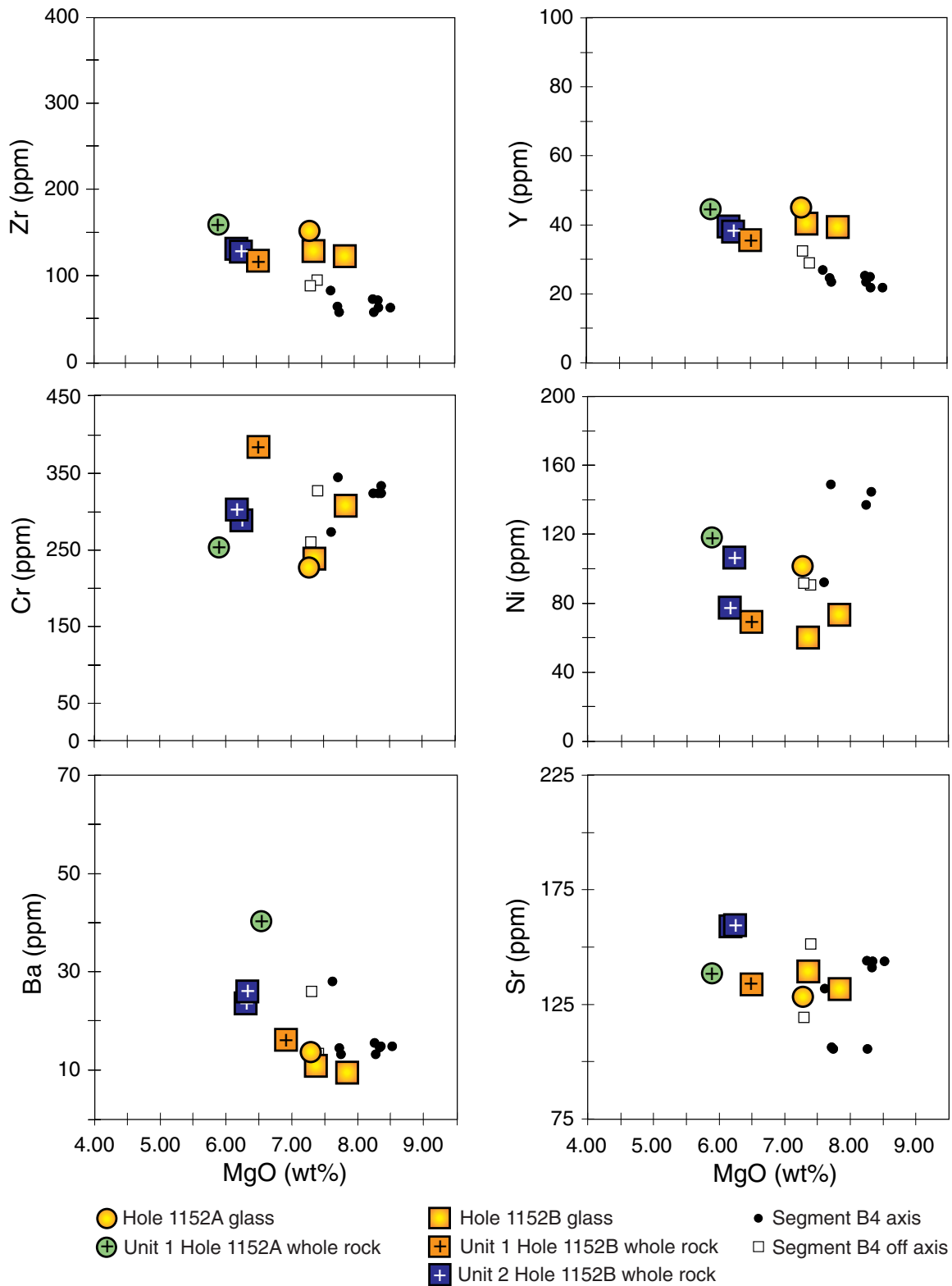


Figure F14. A. Variations of Zr/Ba vs. Ba for Holes 1152A and 1152B basaltic glass and whole-rock Southeast Indian Ridge (SEIR) lavas dredged between 123°E and 133°E. TP = Transitional Pacific; PRT = propagating rift tip. **B.** Variations of Na₂O/TiO₂ vs. MgO for Holes 1152A and 1152B basaltic glass and whole-rock samples compared with Indian- and Pacific-type MORB fields defined by zero-age SEIR lavas dredged between 123°E and 133°E. Dashed line separates Indian- and Pacific-type zero-age SEIR basalt glass.

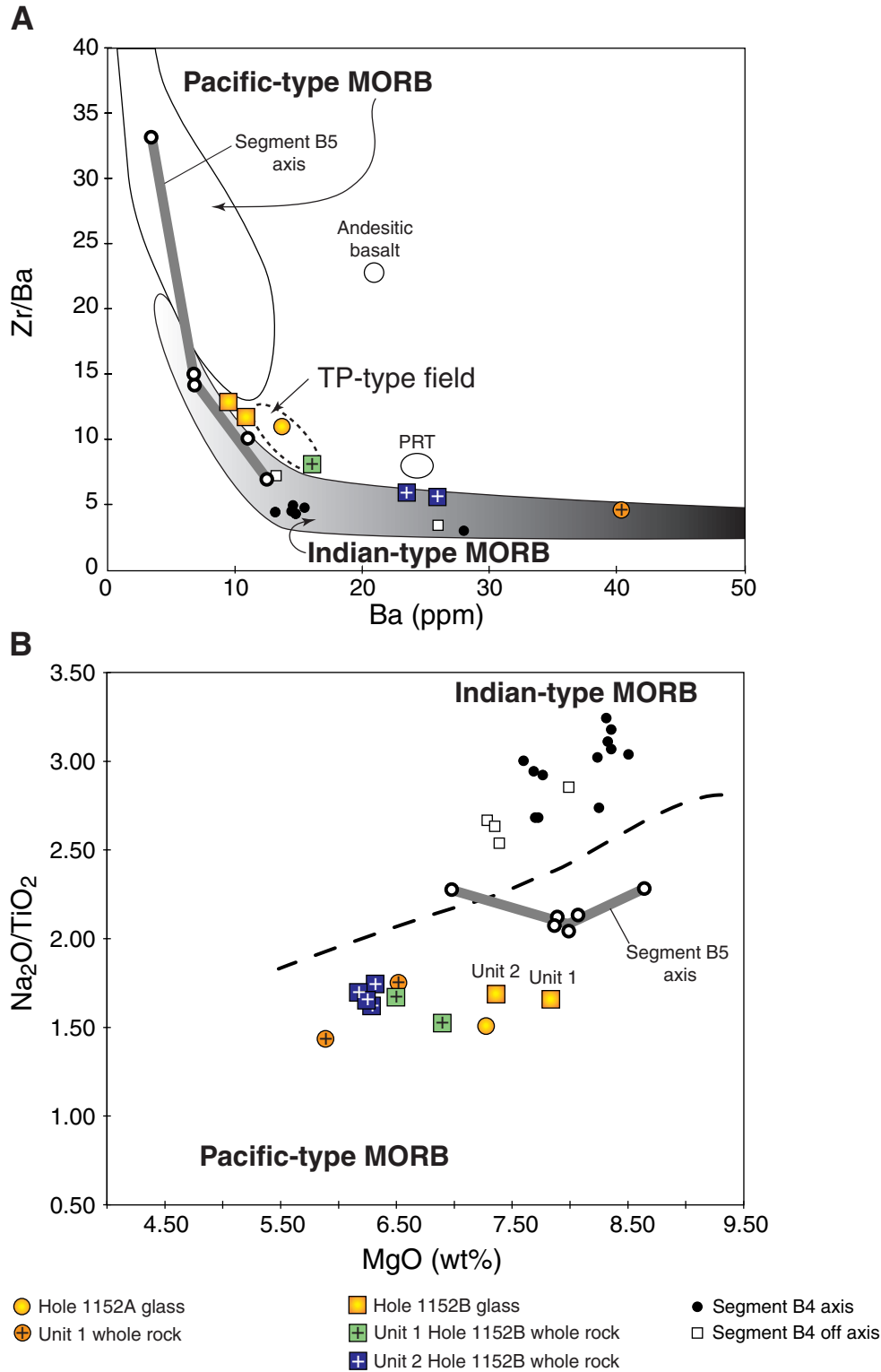


Table T1. Coring summary, Site 1152.

Hole 1152A

Latitude: 41°53.8762'S
 Longitude: 127°0.4032'E
 Time on hole: 1215 hr, 26 Nov 99–1115 hr, 27 Nov 99 (23.00 hr)
 Time on site: 1215 hr, 26 Nov 99–0000 hr, 29 Nov 99 (59.75 hr)
 Seafloor (drill-pipe measurement from rig floor, mbrf): 5066.4
 Distance between rig floor and sea level (m): 11.2
 Water depth (drill-pipe measurement from sea level, m): 5055.2
 Total depth (from rig floor, mbrf): 5077.6
 Total penetration (mbsf): 11.2
 Total length of cored section (m): 11.0
 Total core recovered (m): 0.59
 Core recovery (%): 5.3
 Total number of cores: 1

Hole 1152B

Latitude: 41°53.8329'S
 Longitude: 127°0.4544'E
 Time on hole: 1115 hr, 27 Nov 99–0000 hr, 29 Nov 99 (36.75 hr)
 Seafloor (drill-pipe measurement from rig floor, mbrf): 5066.4
 Distance between rig floor and sea level (m): 11.0
 Water depth (drill-pipe measurement from sea level, m): 5055.4
 Total depth (from rig floor, mbrf): 5112.7
 Total penetration (mbsf): 46.3
 Total length of cored section (m): 23.7
 Total length of drilled intervals (m): 22.6
 Total core recovered (m): 3.59
 Core recovery (%): 15.1
 Total number of cores: 6
 Number of drilled cores: 1

Core	Date (Nov 1999)	Ship local time	Depth (mbsf)		Length (m)		Recovery (%)	Comment
			Top	Bottom	Cored	Recovered		
187-1152A-1R	27	1230	0.0	11.2	11.2	0.59	5.3	
187-1152B-1W	27	1315	0.0	22.6	22.6	0.00	N/A	Drilled interval
2R	27	1830	22.6	27.8	5.2	0.44	8.5	
3R	27	0415	27.8	35.8	8.0	0.13	1.6	
4R	28	0835	35.8	40.8	5.0	1.39	27.8	
5R	28	1100	40.8	45.3	4.5	1.25	27.8	
6R	28	1420	45.3	46.3	1.0	0.38	38.0	
				Cored:	23.7	3.59	15.1	
				Drilled:	22.6			
				Total:	46.3			

Notes: N/A = not applicable. This table is also available in [ASCII](#) format.

Table T2. Summary of lithologic units, Site 1152.

Hole	Unit	Rock name	Cored interval		Alteration	Lava type
			From	To		
1152A	1	Aphyric basalt	1R-1 (Piece 1)	1R-1 (Piece 10)	Slight	Pillow basalt
1152B	1	Aphyric basalt	2R-1 (Piece 1)	4R-1 (Piece 5)	Slight	Pillow basalt
1152B	2	Moderately to sparsely plagioclase phyric basalt	4R-1 (Piece 6)	6R-1 (Piece 7)	Slight	Pillow basalt

Note: This table is also available in [ASCII](#) format.

Table T3. Summary of glass occurrences, Site 1152.

Core, section	Unit	Depth (mbsf)	Glass ± phenocrysts, spherulites	Coalesced spherulites	Variolitic zone
187-1152A-	1				
1R-1 (Piece 4)		0.30		X	X
1R-1 (Piece 6)		0.37		X	X
1R-1 (Piece 8)		0.47	X	X	X
1R-1 (Piece 10)		0.56		X	X
187-1152B-	1				
2R-1 (Piece 1)		22.60		X	X
2R-1 (Piece 4)		22.74	X		
2R-1 (Piece 5)		22.79		X	X
2R-1 (Piece 9)		22.91		X	X
2R-1 (Piece 10)		22.95		X	X
2R-1 (Piece 12)		23.03		X	X
3R-1 (Piece 1)		27.80	X	X	X
187-1152B-	2				
4R-1 (Piece 17)		36.68	X	X	X
4R-1 (Piece 20)		36.79	X	X	X
4R-1 (Piece 22)		36.90	X	X	X
4R-1 (Piece 24)		36.99	X		
5R-1 (Piece 1)		40.80	X	X	X
5R-1 (Piece 12)		41.31	X	X	X
5R-1 (Piece 25)		41.89	X	X	X
6R-1 (Piece 2)		45.34	X	X	X
6R-1 (Piece 3)		45.50	X	X	X

Notes: The depth indicated does not precisely locate the piece in the hole (see "Introduction," p. 4). X = presence of the zone. This table is also available in [ASCII](#) format.

Table T4. Rock samples incubated for enrichment cultures and prepared for DNA analysis and electron microscope studies and microspheres evaluated for contamination.

Core	Depth (mbsf)	Sample type	Enrichment cultures			DNA analysis		SEM/TEM samples	
			Anaerobic	Aerobic	Microcosm*	Wash	Fixed	Fixed	Air dried
187-1152A-1R	0.0-11.2	Rock	3	3	1 Fe/S	X	X	X	X
187-1152B-4R	35.8-40.8	Rock	10	3		X	X		X

Notes: * = microcosm for iron and sulfur (Fe/S) or manganese redox cycles; SEM = scanning electron microscope; TEM = transmission electron microscopy; X = sample prepared on board. This table is also available in [ASCII](#) format.

Table T5. Glass and whole-rock major and trace element compositions of basalts, Site 1152.

Core, section:	Hole 1152A					Hole 1152B													
	1R-1	1R-1	1R-1	1R-1	1R-1	2R-1	2R-1	2R-1	3R-1	3R-1	4R-1	4R-1	4R-1	5R-1	5R-1	5R-1	5R-1	5R-1	
Interval (cm):	30-34	30-34	30-34	60-62	60-62	10-13	10-13	10-13	2-4	2-4	57-61	57-61	57-61	44-47	44-47	44-47	68-74	68-74	
Depth (mbsf):	0.30	0.30	0.30	0.60	0.60	22.70	22.70	22.70	29.82	29.8	36.37	36.37	36.37	41.24	41.24	41.24	41.48	41.48	
Piece:	3	3	3	8	8	2	2	2	1	1	10	10	10	9	9	9	13	13	
Unit:	1	1	1	1	1	1	1	1	1	1	2	2	2	2	2	2	2	2	
Analysis:	XRF	XRF	ICP	ICP	ICP	XRF	XRF	ICP	ICP	ICP	XRF	XRF	ICP	XRF	XRF	ICP	ICP	ICP	
Rock type:	Aphyric basalt			Glass	Glass	Aphyric basalt			Glass	Glass	Moderately plagioclase-clinopyroxene phyric basalt			Moderately plagioclase-clinopyroxene phyric basalt			Glass	Glass	
Major element (wt%)																			
SiO ₂	48.71	48.86	49.60*	50.50	50.12	48.88	49.01	51.70*	51.60	52.36	50.06	50.21	52.76*	49.78	50.43	53.59*	50.90	52.19	
TiO ₂	2.03	2.06	2.13	2.02	2.02	1.54	1.55	1.56	1.68	1.65	1.65	1.68	1.66	1.67	1.70	1.61	1.81	1.81	
Al ₂ O ₃	14.35	14.21	13.69	14.42	14.46	14.54	14.63	14.24	15.09	15.04	15.31	15.49	15.50	15.59	15.58	15.41	14.86	14.74	
Fe ₂ O ₃	11.20	11.14	12.55	11.44	11.60	10.97	10.97	11.41	10.73	10.64	8.48	8.69	8.78	8.94	8.92	9.06	11.16	11.51	
MnO	0.16	0.16	0.18	0.18	0.18	0.16	0.16	0.16	0.16	0.18	0.16	0.17	0.17	0.17	0.17	0.17	0.19	0.19	
MgO	5.89	5.89	6.52	7.32	7.24	6.49	6.51	6.90	7.97	7.71	6.16	6.19	6.32	6.20	6.29	6.29	7.30	7.43	
CaO	10.39	10.40	10.76	10.45	10.29	11.18	11.23	10.88	11.73	11.79	11.54	11.54	11.40	11.51	11.60	10.82	11.48	11.36	
Na ₂ O	2.90	2.97	3.73	3.01	3.08	2.60	2.56	2.38	2.60	2.92	2.83	2.82	2.89	2.74	2.83	2.61	3.02	3.08	
K ₂ O	0.51	0.51	0.58	0.23	0.22	0.57	0.57	0.61	0.16	0.17	0.33	0.33	0.36	0.29	0.30	0.27	0.19	0.18	
P ₂ O ₅	0.23	0.22	0.26	0.24	0.22	0.16	0.16	0.15	0.18	0.18	0.16	0.16	0.17	0.17	0.17	0.16	0.19	0.15	
LOI	1.52	1.52				1.04	1.04				0.21	0.21		0.07	0.07				
CO ₂																			
H ₂ O																			
Total:	97.89	97.94	100.00	99.83	99.43	98.13	98.39	100.00	101.90	102.63	96.89	97.49	100.00	97.13	98.06	100.00	101.09	102.64	
Trace element (ppm)																			
Nb	10	7				8	4				9	6		9	6				
Zr	160	161	191	146	159	118	118	132	118	130	131	133	148	128	130	142	135	124	
Y	44	45	48	45	45	36	35	36	40	38	39	40	39	38	38	39	39	42	
Sr	138	139	147	129	129	134	133	136	135	129	160	158	162	160	159	160	139	141	
Rb	8	9				15	15				3	3		2	3				
Zn	100	101				87	87				95	94		86	87				
Cu	62	62				73	72				64	63		74	74				
Ni	118	119	108	106	97	70	68	63	71	75	78	77	70	107	106	90	58	62	
Cr	250	254	235	232	218	383	382	307	288	322	302	300	261	290	284	225	240	233	
V	328	335				311	313				300	300		304	309				
Ce	42	43				36	33				42	40		39	38				
Ba			40	14	14			16	9	10			26			24	11	11	
Sc				35	39				39	43							42	43	

Notes: Data tables for every site report the XRF major element analysis from two fused disks and trace element analyses from a single pressed-powder pellet, all made from splits of a single sample powder. A split of the same whole-rock powder was also analyzed by ICP-AES for major and trace elements. Reported ICP-AES results are repeated analyses of a single solution measured two or three times during a run. ICP-AES whole-rock data are suspect for Site 1152. However, the glasses have been sampled, dissolved, and analyzed a second time and are considered reliable. * = SiO₂ by difference for ICP-AES; LOI = loss on ignition. This table is also available in [ASCII](#) format.